Exome Sequencing Identifies Mutations in *CCDC114* as a Cause of Primary Ciliary Dyskinesia

Michael R. Knowles,[1,*] Margaret W. Leigh,[2] Lawrence E. Ostrowski,[1] Lu Huang,[1] Johnny L. Carson,[2] Milan J. Hazucha,[1] Weining Yin,[1] Jonathan S. Berg,[1,3] Stephanie D. Davis,[2,13] Sharon D. Dell,[4] Thomas W. Ferkol,[5] Margaret Rosenfeld,[6] Scott D. Sagel,[7] Carlos E. Milla,[8] Kenneth N. Olivier,[9] Emily H. Turner,[10] Alexandra P. Lewis,[10] Michael J. Bamshad,[10,11] Deborah A. Nickerson,[10] Jay Shendure,[10] Maimoona A. Zariwala,[12,*] and the Genetic Disorders of Mucociliary Clearance Consortium

Primary ciliary dyskinesia (PCD) is a genetically heterogeneous, autosomal-recessive disorder, characterized by oto-sino-pulmonary disease and situs abnormalities. PCD-causing mutations have been identified in 14 genes, but they collectively account for only ~60% of all PCD. To identify mutations that cause PCD, we performed exome sequencing on six unrelated probands with ciliary outer dynein arm (ODA) defects. Mutations in *CCDC114*, an ortholog of the *Chlamydomonas reinhardtii* motility gene *DCC2*, were identified in a family with two affected siblings. Sanger sequencing of 67 additional individuals with PCD with ODA defects from 58 families revealed *CCDC114* mutations in 4 individuals in 3 families. All 6 individuals with *CCDC114* mutations had characteristic oto-sino-pulmonary disease, but none had situs abnormalities. In the remaining 5 individuals with PCD who underwent exome sequencing, we identified mutations in two genes (*DNAI2*, *DNAH5*) known to cause PCD, including an Ashkenazi Jewish founder mutation in *DNAI2*. These results revealed that mutations in *CCDC114* are a cause of ciliary dysmotility and PCD and further demonstrate the utility of exome sequencing to identify genetic causes in heterogeneous recessive disorders.

Primary ciliary dyskinesia (PCD) is a rare, autosomal-recessive disorder (MIM 244400) of motile cilia structure and/or function (incidence, ~1:16,000). Clinical features include respiratory distress in term neonates, onset of chronic cough and middle ear disease early in life, chronic rhinosinusitis, age-dependent bronchiectasis, defective sperm motility/infertility in males, and laterality defects in 50% of affected individuals (see References[1–5] and GeneReviews in Web Resources). The diagnosis of PCD has traditionally relied on transmission electron microscopy (EM) to demonstrate different types of ultrastructural defects in cilia (for example, outer and/or inner dynein arm defects and/or central apparatus defects) as we and others have reported (see References[2–10] and GeneReviews in Web Resources).

PCD is highly genetically heterogeneous, and mutations in 14 known genes collectively account for just ~60% of cases. Interestingly, mutations of each known gene are linked to a specific ciliary ultrastructural phenotype (reviewed in GeneReviews, Zariwala et al.,[2] Chilvers et al.[11]). We speculated that studying individuals with the same ciliary phenotype (ultrastructural defect) would facilitate the identification of additional mutations in genes underlying PCD; therefore, we performed exome sequencing of six unrelated individuals with isolated outer dynein arms (ODA) defects, which is the most common ciliary phenotype in PCD (see References[2,6–10] and GeneReviews in Web Resources). Clinical, phenotypic, and demographic information of these six individuals, including levels of nasal nitric oxide (nNO), which are very low in PCD,[3,5,9,12] are presented (Table 1 and Table S1 available online). To enhance the likelihood of identifying mutations in additional gene(s), we selected for exome sequencing only those individuals in whom mutations in the two genes (*DNAH5* [MIM 603335]; *DNAI1* [MIM 604366]) most frequently associated with ODA defects (see References[2,13–15] and GeneReviews in Web Resources) had been excluded by Sanger sequencing.

The study was approved by the Committee for the Protection of the Rights of Human Subjects at the UNC and participating institutions, and written consent was obtained.

Exome sequencing was performed as previously described.[16] The Nimblegen EZ SeqCap kit (Roche) was used to capture exons. Shotgun libraries were constructed by shearing DNA and ligating sequencing adaptors bearing

[1]Department of Medicine, UNC School of Medicine, Chapel Hill, NC 27599, USA; [2]Department of Pediatrics, UNC School of Medicine, Chapel Hill, NC 27599, USA; [3]Department of Genetics, UNC School of Medicine, Chapel Hill, NC 27599, USA; [4]Child Health Evaluative Sciences, Research Institute, The Hospital for Sick Children, Toronto, ON M5G 1X8, Canada; [5]Department of Pediatrics, Washington University School of Medicine, St. Louis, MO 63110, USA; [6]Children's Hospital and University of Washington, Seattle, WA 98105, USA; [7]Department of Pediatrics, University of Colorado School of Medicine, Aurora, CO 80045, USA; [8]Department of Pediatrics, Stanford University, Stanford, CA 94304, USA; [9]Laboratory of Clinical Infectious Diseases, National Institute of Allergy and Infectious Diseases, Bethesda, MD 20892, USA; [10]Department of Genome Sciences, University of Washington School of Medicine, Seattle, WA 98195, USA; [11]Department of Pediatrics, University of Washington School of Medicine, Seattle, WA 98195, USA; [12]Department of Pathology & Laboratory Medicine, UNC School of Medicine, Chapel Hill, NC 27599, USA
[13]Present address: Section of Pediatric Pulmonology, Allergy and Sleep Medicine, James Whitcomb Ruket Riley Hospital for Children, Indiana University School of Medicine, Indianapolis, IN 46202, USA
*Correspondence: knowles@med.unc.edu (M.R.K.), zariwala@med.unc.edu (M.A.Z.)
http://dx.doi.org/10.1016/j.ajhg.2012.11.003.

Table 1. Demographic, Clinical, and *CCDC114* Mutations in Six PCD-Affected Individuals from Four Unrelated Families

Individual #	Family #	Sex	Age in Years	Situs Status	Ciliary Ultra-structural Defect	Ethnicity	nNO nl/min[a]	Neo RDS	Bxsis	Sinusitis	Otitis Media	Allele 1				Allele 2			
												Exon/ Intron	Base Change	Amino Acid Change	Segre-gation[b]	Exon/ Intron	Base Change	Amino Acid Change	Segre-gation[b]
Homozygous Mutations																			
#359[c]	UNC-62	F	39	SS	ODA	white	36.0	yes	yes	yes	yes	Ex 7	c.742G>A[d]	p.Ala248Serfs*52	paternal[c]	Ex 7	c.742G>A[d]	p.Ala248Serfs*52	maternal
#360[c]	UNC-62	F	33	SS	ODA	white	31.5	yes	yes	yes	yes	Ex 7	c.742G>A[d]	p.Ala248Serfs*52	paternal[c]	Ex 7	c.742G>A[d]	p.Ala248Serfs*52	maternal
Compound Heterozygous Mutations																			
#891	UNC-139	F	59	SS	ODA	white	32.4	yes	yes	yes	yes	Ex 7	c.742G>A[d]	p.Ala248Serfs*52	NA[e]	Int 5	c.487−2A>G[d]	p.Glu163Glyfs*60, p.Glu163_ Val184delins[g]	NA[e]
#897	UNC-140	M	3	SS	ODA	white	9.6	yes	no	no	yes	Ex 7	c.742G>A[d]	p.Ala248Serfs*52	maternal	Int 12	c.1391+5G>A[d]	p.Ser432Argfs*7	paternal
#1107	UNC-212	F	34	SS	ODA	white	5.5	no	yes	yes	yes	Ex 7	c.742G>A[d]	p.Ala248Serfs*52	maternal[f]	Ex 9	c.939delT	p.His313Glnfs*14	paternal
#1114	UNC-212	F	38	SS	NA	white	NA	no	NA	NA	yes	Ex 7	c.742G>A[d]	p.Ala248Serfs*52	maternal[f]	Ex 9	c.939delT	p.His313Glnfs*14	paternal

Abbreviations: M, male; F, female; SI, situs inversus; SA, situs ambiguous; SS, situs solitus; NA, not available; ODA, outer dynein arms; Neo RDS, neonatal respiratory distress in full-term birth; Bxsis, bronchiectasis; nNO, nasal nitric oxide.

[a]Normal nNO levels are 376 ± 124 nl/min (mean ± SD), calculated from 27 healthy subjects.[3]

[b]Mutant allele shown to segregate with either the father's (paternal) or mother's (maternal) side of the family.

[c]DNA from father was not available, but paternal aunt carried the mutation and hence father was an obligate carrier, see details in Figure 1 showing segregation analysis.

[d]Splice-site mutations interrogated with RT-PCR, see details in Table 2.

[e]Three unaffected siblings of the affected individual, each carried only one mutation representing *trans* inheritance, see details in Figure 1 showing segregation analysis.

[f]DNA from father was not available, but mother carried the other mutation so father is an obligate carrier, see details in Figure 1 showing segregation analysis.

[g]Two transcripts were observed predicting two different translation products.

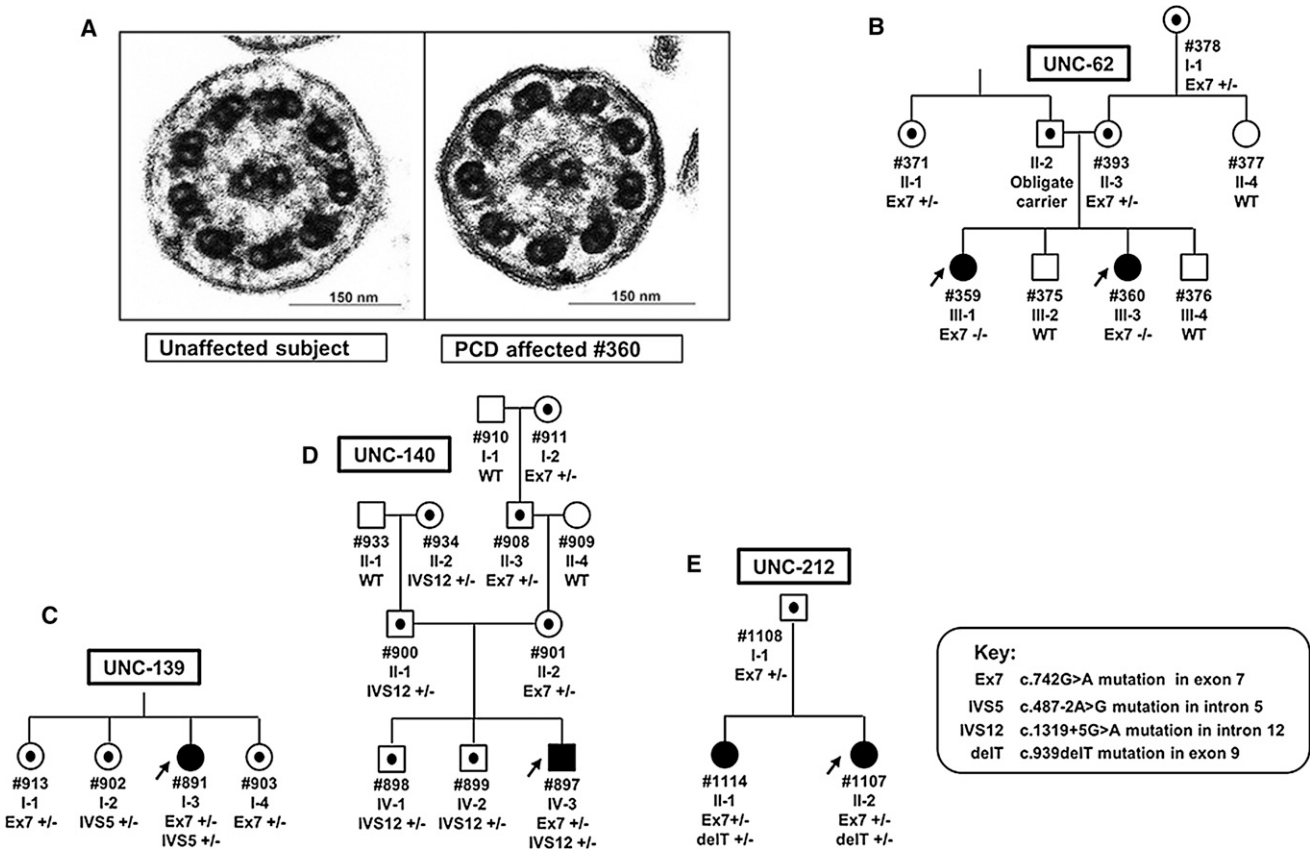

Figure 1. Cross-section Analysis of Ciliary Ultrastructure by Electron Microscopy and Segregation Analysis of *CCDC114*
(A) Normal ciliary ultrastructure from healthy subject (left) and absence of outer dynein arms (right) from UNC family 62 with biallelic mutations in *CCDC114*.
(B–E) Pedigrees with mutations segregating in *trans*, consistent with autosomal-recessive mode of inheritance.

an 8 base pair barcode, followed by PCR amplification. Libraries were hybridized to EZSeqCap V1 (corresponding to CCDS2008 gene set) solution-based probe, amplified, pooled, and sequenced on Illumina GAIIx (PE76 + barcode read). The final targeted region was 26,402,573 bp that included 16,151 genes (198,334 exons and splice junctions). The average mean fold coverage was 84×; ~98% target bases were covered at least at 1× and ~93% covered at 8×. The details of capture statistics and coverage are presented in Table S2. After barcode-based sample deconvolution, sequence reads were mapped with BWA tools to the human genome (hg18). Sequence variant calls were performed by SAMtools after removing potential PCR duplicates, with a minimum quality threshold of 30 for SNPs and 200 for indels. On average we called 18,235 base substitutions and 578 insertions/deletions per individual (Table S2). Genotypes were annotated with the SeattleSeq server (Table S3). Missense-, nonsense-, or splice-site-altering variants absent from 1000 Genomes data and also absent or at a minor allele frequency (MAF) of <1% in other exomes sequenced at the University of Washington (n = 849) were considered further, as were indels that were absent or observed <10 times in the other exomes sequenced at the University of Washington. Under an autosomal-recessive model for PCD, only genes with biallelic variants (homozygous or compound heterozygous) were considered further (Tables S2 and S3). We manually checked each of these variants for its potential of being pathogenic, highlighting a subset for validation by Sanger sequencing. Candidate genes were prioritized for validation by Sanger sequencing (Tables S3 and S4), based on expression in ciliated airway epithelia (RNA-seq data set, unpublished) and potential relevance to PCD as assessed through published information, including analysis of large-scale coexpression data sets.[17,18] The primer sequences and results of validation are depicted in Tables S3 and S4. For the potentially pathogenic variants in a proband, segregation analysis on the available DNA from the relatives was carried out.

An apparently homozygous missense variant (c.742G>A) was identified in *CCDC114* (RefSeq: NM_144577.3) at the last base of exon 7 in an individual with PCD with ODA defect (Figure 1A), altering the protein sequence and potentially affecting splicing. Sanger sequencing confirmed inheritance in *trans* for the propositus and an affected sibling, and two unaffected siblings had no mutation (Figure 1B). The *CCDC114* ortholog in *Chlamydomonas reinhardtii, DCC2* (*oda-DC2*),[19] encodes a component of the outer dynein arm docking complex, and a *Chlamydomonas* mutant in *DCC2* (*oda1.1*) has

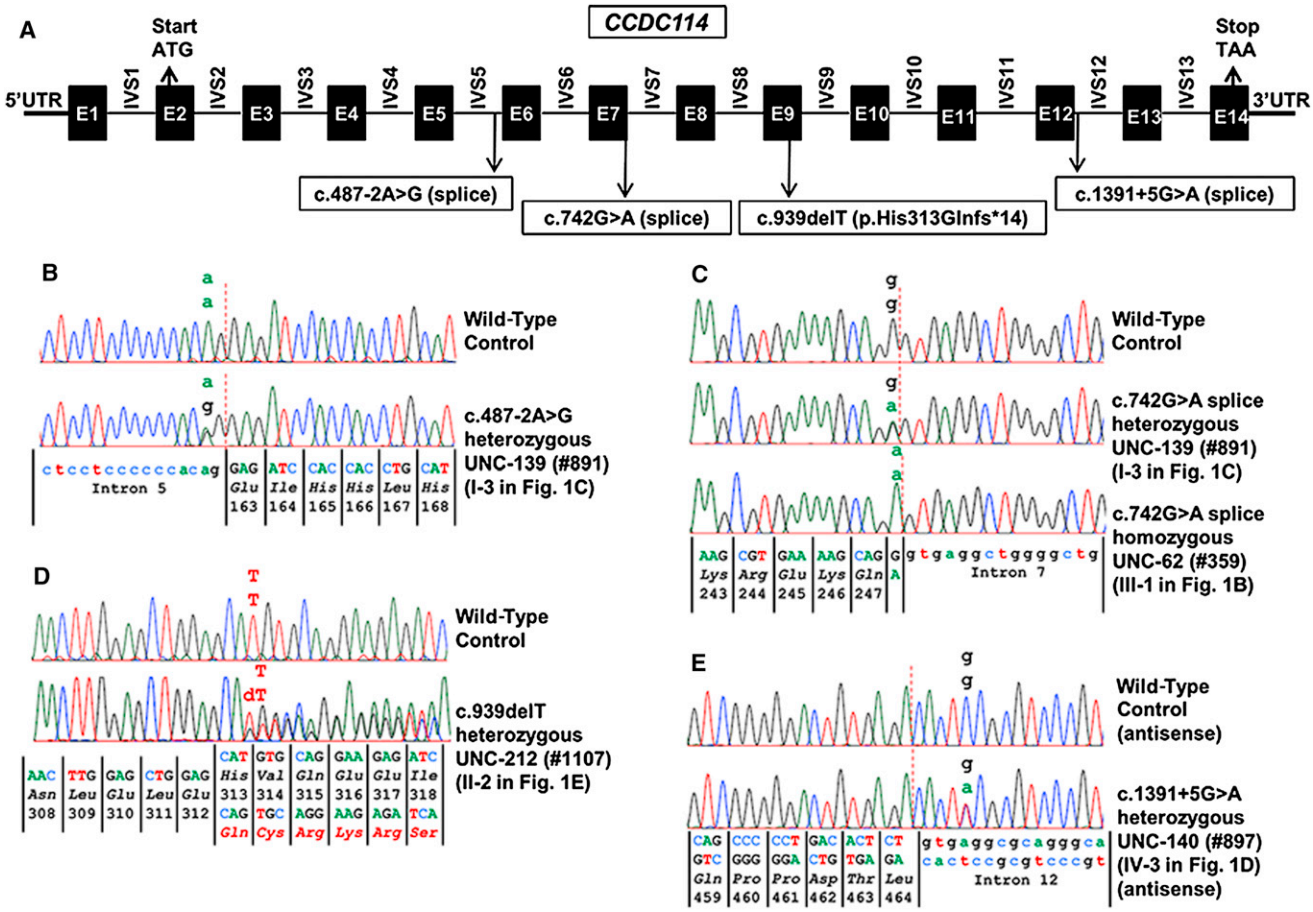

Figure 2. Genomic Organization of *CCDC114* and Location of PCD-Causing Mutations
(A) The transcript of *CCDC114* consists of 3,215 bp and encodes 670 amino acid protein. Filled box designates exons "E," horizontal lines designate intron "IVS," and location of 5′ UTR, 3′ UTR, and start and stop codons are shown. Introns/exons are not drawn to scale. The positions of all identified *CCDC114* mutations are indicated.
(B, D, and E) Heterozygous sequences in affected (bottom) and corresponding wild-type (top) sequences in controls.
(C) Homozygous (bottom) and heterozygous (middle) sequences in affected and the corresponding wild-type sequences (top) in control. Base sequence, amino acid sequence, and codon numbers are shown. Intron-exon junctions are shown with the red dotted lines.

impaired motility and ODA defects analogous to the ultrastructural defect in PCD. Therefore, we performed high-throughput Sanger-based sequencing of *CCDC114* (Genotyping and Resequencing Services in Seattle; RC2-HL-102923; MJB-primer sequences: Table S5) in 104 additional individuals with PCD from 91 families (67 affected individuals from 58 families with isolated ODA defects; 37 affected individuals from 33 families with ODA+IDA defects) (Table S6). Four individuals from three families with isolated ODA defects had biallelic mutations in *CCDC114,* including two affected siblings (UNC family 212) (Table 1). Segregation analysis at UNC by Sanger sequencing (capillary electrophoresis; Applied Biosystems, Foster City, CA) confirmed that the mutations were inherited in *trans* (Table 1, Figures 1C–1E). In total, there were four different mutations (three splice-site and one frameshift) in four unrelated families.

The c.742G>A splice-site variant was found in each unrelated PCD family: homozygous in one family and compound heterozygous in three families harboring a different splice-site or frameshift mutation on the second allele (Table 1). The genomic organization of *CCDC114* and location of mutations is shown (Figure 2). The finding that c.742G>A is a rare PCD-causing variant is consistent with the observation that this splice mutation is present at very low frequency on the NHBLI Exome Variant Server (EVS) (3 of 7,020 alleles; 0.043%) in non-PCD subjects of European ancestry, as compared with our 64 families with isolated ODA defects (5 of 128 alleles; 3.9%). The presence of likely causative mutations in EVS indicates that the depth of publicly available data for genetic variation is now sufficiently deep that caution must be exercised when filtering exome or genome data, particularly for recessive disorders. Neither intronic splice mutations (c.487−2A>G, c.1391+5G>A) nor the frameshift mutation (c.939delT) was present in either dbSNP or EVS. For subjects harboring the c.742G>A mutation, we constructed haplotypes for all variants/polymorphisms in *CCDC114* and found that all affected individuals carried a conserved haplotype in *cis* with the c.742G>A mutation,

Table 2. Effect of *CCDC114* Splice-Site Mutations on cDNA Transcript via Reverse-Transcriptase PCR in Individuals with PCD

Primer Set[a]	Mutation Intron/ Exon Location	Genomic Mutations (Predicted Amino Acid Change)	cDNA Transcript after RT-PCR (Predicted Amino Acid Change)	Comments
exons 4 sense + 10 antisense	exon 7[b]	c.742G>A (p.Ala248Thr)	mutant 1: r.742+1_742+79ins (p.Ala248Serfs*52)	Mutant 1 had insertion of 79 bp from start of intron 7 followed by cryptic splice donor site and addition of exon 8. Wild-type amplification product: 657 bp. Mutant amplification product: 736 bp.
			mutant 2: r.554+1_554+98ins; 742+1_742+79ins (p.Glu186*)	Mutant 2 had insertion of 98 bp from start of intron 6 followed by cryptic splice donor site and addition of exon 7, as well as insertion of 79 bp from start of intron 7 followed by cryptic splice donor site and addition of exon 8. Wild-type amplification product: 657 bp. Mutant amplification product: 834 bp.
exons 10 sense + 13 antisense	exon 7[c]	c.742G>A (p.Ala248Thr)	mutant: r.1129+1283_1129+1410ins	Mutant had insertion of 128 bp from the middle of intron 10 due to cryptic splice donor and acceptor sites following exon 10. The mutant transcript was in *cis* with T allele for c.1403C>T (p.Pro468Leu) polymorphism; proxy for c.742G>A mutation indicating transcript was caused by this mutation. Wild-type amplification product: 479 bp. Mutant amplification product: 607 bp.
exons 4 sense + 10 antisense	intron 5[d]	c.487−2A>G (g.IVS5−2A>G)	mutant 1: r.487_554del (p.Glu163Glyfs*60)	Mutant 1 had deletion of all 68 bp of exon 6 followed by joining of exons 5 and 7. Wild-type amplification product: 657 bp. Mutant amplification product: 589 bp.
			mutant 2: r.487−1_487−59ins; 487_554del (p.Glu163_Val184delins)	Mutant 2 had insertion of 59 bp from the end of intron 6 as well as deletion of all 68 bp of exon 6 leading to in-frame deletion of 22 amino acids that are replaced by insertion of 19 mutant amino acids. Wild-type amplification product: 657 bp. Mutant amplification product: 648 bp.
exons 10 sense + 13 antisense	intron 12	c.1391+5G>A (g.IVS12+5G>A)	mutant: r.1294_1391del (p.Ser432Argfs*7)	Out-of-frame deletion of exon 12 leading to premature translation termination signal. Wild-type amplification product: 479 bp. Mutant amplification product: 381 bp.

[a]Primer sequences depicted in Table S8. RT-PCR was carried out on ciliated epithelia cells collected from inferior nasal turbinate as shown previously.[14]
[b]Two mutant transcripts, both causing frameshift leading to premature translation termination signal, were identified for c.742G>A mutation that is located on the last base in exon 7 on conserved splice donor site in UNC-139 (#891) (I-3 in Figure 1C) as depicted in Figure S2. Only mutant transcript 1 was identified in both siblings in UNC-62 who carried homozygous c.742G>A mutation.
[c]Amplification with primer set exons 4 sense + 13 antisense in individuals with homozygous c.742G>A mutation yielded two major products probably representing the inclusion of intron 7 ± the inclusion of intron 10. Analysis of other individuals by RT-PCR and agarose gel electrophoresis (data not shown) indicated the presence of mutant transcripts with insertion of part of intron 10 in all affected individuals carrying c.742G>A mutation. Irrespective of whether all mutant transcripts resulting from c.742G>A mutations occur with insertion of parts of introns 6, and/or 7, and/or 10, they all cause frameshift leading to premature translation termination signal.
[d]Two mutant transcripts were identified for g.IVS5−2A>G mutation in UNC-139 (#891) (I-3 in Figure 1C) as depicted in Figure S4. This individual had c.742G>A mutation on the *trans* allele, but both mutant transcripts were wild-type at c.742G>A locus, indicating that both these transcripts are caused by g.IVS5−2A>G mutation.

compatible with being a founder mutation (Figure S1). Multiple benign variants are listed that were identified in *CCDC114* (Table S7).

To determine the effect of splice variants in *CCDC114*, reverse-transcriptase polymerase chain reaction (RT-PCR) was performed on RNA from nasal epithelia of individuals with biallelic mutations with cyclophilin as a control (primer sequences: Table S8). The exonic splice-site mutation c.742G>A (present on at least one allele in six individuals from four families) yielded two mutant transcripts, both resulting in premature translation termination signals (Table 2, Figure S2). Using a different downstream primer set revealed another splicing defect on the same mutant allele, indicating impairment of splicing distal to the mutation, as well (Table 2, Figure S3). The aberrant splicing that is three exons downstream from c.742G>A could not compensate for the upstream frameshift, as the upstream insertions lead to termination codons before the inclusion of intron 10. The c.487−2A>G (g.IVS5−2A>G) mutation also yielded two mutant transcripts, one causing premature

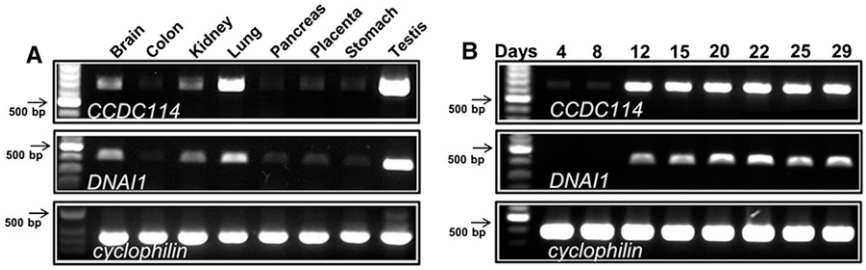

Figure 3. Expression Analysis via Reverse-Transcriptase PCR

(A) Expression pattern of *CCDC114* in a panel of normal human tissues.

(B) Expression pattern of *CCDC114* (top) during ciliogenesis in human airway cells. RNA was isolated from human airway epithelia cells at different times after plating on collagen-coated culture inserts at an air/liquid interface. Under these conditions the cells initially grow as a single monolayer of undifferentiated "basal-like" cells. After 10–14 days, ciliated cells begin to appear, increasing over the next 2–3 weeks before plateauing at approximately 60%–80% of the culture.[21,22] For both expression analyses, *DNAI1* (middle) was used as a known ciliary gene control and cyclophilin (bottom) as a positive RNA control.

translation termination signals and another causing in-frame deletion of exon 6 and inclusion of part of intron 6 (Table 2, Figure S4). The intron 12 splice mutation (c.1391+5G>A [g.IVS12+5G>A]) caused an out-of-frame deletion of exon 12 and a premature translation termination signal (Table 2, Figure S5).

Although 51 individuals with PCD with situs abnormalities underwent *CCDC114* mutation analysis (Table S6), none had mutations. This suggests that *CCDC114* mutations do not affect embryonic nodal cilia motility, and/or that the splice mutant (c.742G>A) is leaky, rendering partial function. Consistent with this, there was faint amplification of full-length mRNA (confirmed by Sanger sequencing) in nasal epithelial RNA from an individual (#359, III-1 in Figure 1B) homozygous for c.742G>A (Figure S6). Despite this leakiness, clinical features and nasal nitric oxide values in individuals with *CCDC114* mutations (Table 1) are indistinguishable from individuals with "classic" PCD with ODA defects and mutations in *DNAI1* and *DNAH5*.[13–15,20] *CCDC114* is highly expressed in testis (Figure 3) and males with PCD are frequently infertile. However, the only male patient in this study is currently 7 years old, which precludes study of fertility or sperm motility.

Genetic data indicating that *CCDC114* mutations recessively cause PCD was robustly supported by additional biological studies. (1) *CCDC114* shows a similar pattern of expression (e.g., high in lung and testis) as *DNAI1*, mutations in which cause PCD with ciliary ODA defects[14] (Figure 3A). (2) *CCDC114* expression in cultured human bronchial cells[21,22] over 30 days parallels the time course of ciliary differentiation and *DNAI1* expression (Figure 3B). (3) Quantitative proteomic analysis of isolated human cilia by data-independent mass spectrometry (LC/MS^E)[23,24] demonstrate that CCDC114 is present in equimolar amounts as DNAI1, mutations in which cause PCD. (4) Videomicroscopy analysis of nasal epithelial cilia obtained by nasal-scrape biopsy from five individuals with biallelic mutations in *CCDC114* showed complete ciliary immotility in most ciliated cells and stiff dyskinetic cilia in some cells.[11,25] When activity was sufficient to quantify ciliary beat frequency, it was reduced compared to normal (average 3.1 Hz versus 7.3 ± 1.5 [SD] Hz at 25°C)[25] (Movies S1, S2, and S3).

The identification of mutations in *CCDC114* as PCD causing is also congruent with other information. (1) The *Chlamydomonas reinhardtii* motility mutant *oda1.1* is defective in *DCC2*,[19] an ortholog of *CCDC114*. Interestingly, the *oda1.1* mutant displays a reduced beat frequency, but is not immotile, suggesting that the absence of outer dynein arms has different functional consequences in these two organisms (human and *Chlamydomonas*). (2) There is coordinate regulation between *CCDC114* and other known genes harboring mutations causing PCD (gene expression data set; UGET).[17,18] (3) Three other members of the coiled-coil domain containing (*CCDC*) family of genes (*CCDC39* [MIM 613798], *CCDC40* [MIM 613799], *CCDC103* [MIM 614677]) are known to play a role in assembly of ciliary inner dynein arms, dynein regulatory complexes, and outer dynein arms, and mutations in these CCDC genes cause PCD.[26–29] (4) *CCDC114* has never been associated with any other genetic disorder.

For the five remaining individuals with PCD with ODA defects who had exome sequencing, three individuals of Ashkenazi Jewish ethnicity had identical homozygous nonsense (c.1304G>A [p.Trp453*]) mutations in *DNAI2* (MIM 605483; RefSeq: NM_023036.4) that were inherited in *trans* (Figure S7). Other mutations in *DNAI2* have been reported as a rare cause of PCD with ODA defects.[30] All three individuals shared a ~158 kb haplotype in *cis* with c.1304G>A, indicative of a founder event (Figure S8). Exome sequencing also identified two mutations in *DNAH5* (RefSeq: NM_001369.2) in an individual with PCD who previously did not have biallelic mutations identified by Sanger sequencing. The two mutants were a 1 bp insertion in exon 16 (c.2261_2262insT [p.Met754Ilefs*5]) and a missense variant (c.6249G>A [p.Met2083Ile]) at the last base of exon 37. Review of the original Sanger sequencing primers for exon 16 revealed a rare variant at the 3′ end of the original antisense primer binding site, thereby causing the allele dropout (Figure S9A). Both mutations were present in an affected sibling, and each parent was a carrier (Figures S9B–S9D). RT-PCR of nasal RNA demonstrated the exon 37 (c.6249G>A) mutation affected splicing, leading to premature translation termination signal (Figure S10). This illustrates that mutations missed by Sanger sequencing may be

identified by different techniques and that retesting of exon 16 may be appropriate, if biallelic mutations in *DNAH5* were not identified by Sanger sequencing with the published primer set.[20] In one individual of Asian-Indian descent with PCD, two missense variants in *DNAH5* were identified by exome sequencing and confirmed by Sanger sequencing: c.1121T>C (p.Ile374Thr) in exon 9 and c.3139G>A (p.Gly1047Arg) in exon 20. The variants were inherited in *trans* (Figures S11A–S11C), and the amino acids were well conserved across species (Figure S11D). In silico mutation prediction analysis (Mutation Taster)[31] scored them as deleterious and both are very rare in public databases, but further genetic and/or functional studies will be necessary to confirm the role of these variants in PCD.

In conclusion, exome sequencing identified mutations in *CCDC114* as a cause of PCD in ~6% of individuals with PCD and an ODA defect. Additionally, we identified a nonsense mutation in *DNAI2* that appears to be a founder mutation in individuals with PCD with Ashkenazi Jewish ethnicity. The identification of genetic causes of PCD in six families via exome sequencing further demonstrates the power of this approach for identifying the etiology in genetically heterogeneous disorders.

Supplemental Data

Supplemental Data include 11 figures, 8 tables, and 3 movies and can be found with this article online at http://www.cell.com/AJHG/.

Acknowledgments

We are grateful to PCD patients and families for their participation. We thank Michele Manion and the US PCD Foundation, all investigators and the coordinators of the Genetic Disorders of Mucociliary Clearance Consortium (GDMCC) that is part of the Rare Disease Clinical Research Network, including Andrea Henkel (NIAID/NIH, MD), Jeffrey Atkinson and Jane Quante (Washington University, MO), Shelley Mann (The Children's Hospital, CO), Sharon McNamara (Children's Hospital, WA), Jacquelyn Zirbes (Stanford University Medical Center, CA), Melody Miki (The Hospital for Sick Children, Toronto, ON, Canada), and Susan Minnix and Caroline O'Connor (UNC-Chapel Hill). We thank Kimberly Burns, Whitney Wolf, Rhonda Pace, and Andrew Cutting for technical assistance; Elizabeth Godwin for administrative support; and Syanne Olson for editorial assistance. We acknowledge Lucy Morgan (Concord Hospital, Australia), Robbert de Iongh (University of Melbourne, Australia), and Ugo Pradal (Cystic Fibrosis Center, Verona, Italy) for providing DNA.

Funding support for research was provided to M.R.K., M.W.L., J.L.C., M.J.H., S.D. Davis, S.D. Dell, T.W.F., K.N.O., S.D.S., M.R., C.E.M., and M.A.Z. by US NIH/ORDR/NHLBI grant 5U54 HL096458-06, to M.R.K., L.E.O., and M.A.Z. by NIH-NHLBI grant 5R01HL071798, to J.S. and D.A.N. by NIH-NHLBI grant 5R01HL094976, to M.J.B. by NIH-NHLBI grant RC2 HL-102923, and to J.S. by NIH/NHGRI grant 5R21HG004749 and NIH/NCATS grants UL1 TR000083, UL1 TR000154, and CFF R026-CR07. In addition, this publication was made possible by grants from the ORDR, NHLBI, NHGRI, and NCATS, components of NIH. Its contents are solely the responsibility of the authors and do not necessarily represent the official view of NIH.

Received: August 21, 2012
Revised: September 20, 2012
Accepted: November 1, 2012
Published: December 20, 2012

Web Resources

The URLs for data presented herein are as follows:

1000 Genomes, http://browser.1000genomes.org/index.html
dbGaP, http://www.ncbi.nlm.nih.gov/gap
dbSNP, http://www.ncbi.nlm.nih.gov/projects/SNP/
Ensembl Genome Browser, http://www.ensembl.org/index.html
GeneReviews, Zariwala, M., Knowles, M., and Leigh, M.W. (2012). Primary ciliary dyskinesia, http://www.ncbi.nlm.nih.gov/books/NBK1122
Genetic Disorders of Mucociliary Clearance Consortium (GDMCC), http://rarediseasesnetwork.epi.usf.edu/gdmcc/index.htm
Mutation Taster, http://neurocore.charite.de/MutationTaster/index.html
NHLBI Exome Variant Server/Sequencing Project (ESP), http://evs.gs.washington.edu/EVS/
Online Mendelian Inheritance in Man (OMIM), http://www.omim.org/
RefSeq, http://www.ncbi.nlm.nih.gov/RefSeq
RS&G NHLBI Resequencing and Genotyping Service, http://rsng.nhlbi.nih.gov/scripts/index.cfm
SeattleSeq Annotation 137, http://snp.gs.washington.edu/SeattleSeqAnnotation137/
UCLA Gene Expression Tool (UGET), http://genome.ucla.edu/~jdong/GeneCorr.html
UCSC Genome Browser, http://genome.ucsc.edu

References

1. Leigh, M.W., Pittman, J.E., Carson, J.L., Ferkol, T.W., Dell, S.D., Davis, S.D., Knowles, M.R., and Zariwala, M.A. (2009). Clinical and genetic aspects of primary ciliary dyskinesia/Kartagener syndrome. Genet. Med. *11*, 473–487.
2. Zariwala, M.A., Knowles, M.R., and Omran, H. (2007). Genetic defects in ciliary structure and function. Annu. Rev. Physiol. *69*, 423–450.
3. Noone, P.G., Leigh, M.W., Sannuti, A., Minnix, S.L., Carson, J.L., Hazucha, M., Zariwala, M.A., and Knowles, M.R. (2004). Primary ciliary dyskinesia: diagnostic and phenotypic features. Am. J. Respir. Crit. Care Med. *169*, 459–467.
4. Kennedy, M.P., Omran, H., Leigh, M.W., Dell, S., Morgan, L., Molina, P.L., Robinson, B.V., Minnix, S.L., Olbrich, H., Severin, T., et al. (2007). Congenital heart disease and other heterotaxic defects in a large cohort of patients with primary ciliary dyskinesia. Circulation *115*, 2814–2821.
5. Bush, A., Chodhari, R., Collins, N., Copeland, F., Hall, P., Harcourt, J., Hariri, M., Hogg, C., Lucas, J., Mitchison, H.M., et al. (2007). Primary ciliary dyskinesia: current state of the art. Arch. Dis. Child. *92*, 1136–1140.
6. Carlén, B., and Stenram, U. (2005). Primary ciliary dyskinesia: a review. Ultrastruct. Pathol. *29*, 217–220.

7. Escudier, E., Couprie, M., Duriez, B., Roudot-Thoraval, F., Millepied, M.C., Prulière-Escabasse, V., Labatte, L., and Coste, A. (2002). Computer-assisted analysis helps detect inner dynein arm abnormalities. Am. J. Respir. Crit. Care Med. *166*, 1257–1262.
8. Jorissen, M., Willems, T., Van der Schueren, B., Verbeken, E., and De Boeck, K. (2000). Ultrastructural expression of primary ciliary dyskinesia after ciliogenesis in culture. Acta Otorhinolaryngol. Belg. *54*, 343–356.
9. Leigh, M.W., O'Callaghan, C., and Knowles, M.R. (2011). The challenges of diagnosing primary ciliary dyskinesia. Proc. Am. Thorac. Soc. *8*, 434–437.
10. Olin, J.T., Burns, K., Carson, J.L., Metjian, H., Atkinson, J.J., Davis, S.D., Dell, S.D., Ferkol, T.W., Milla, C.E., Olivier, K.N., et al.; for the Genetic Disorders of Mucociliary Clearance Consortium. (2011). Diagnostic yield of nasal scrape biopsies in primary ciliary dyskinesia: A multicenter experience. Pediatr. Pulmonol. *46*, 483–488.
11. Chilvers, M.A., Rutman, A., and O'Callaghan, C. (2003). Ciliary beat pattern is associated with specific ultrastructural defects in primary ciliary dyskinesia. J. Allergy Clin. Immunol. *112*, 518–524.
12. Narang, I., Ersu, R., Wilson, N.M., and Bush, A. (2002). Nitric oxide in chronic airway inflammation in children: diagnostic use and pathophysiological significance. Thorax *57*, 586–589.
13. Hornef, N., Olbrich, H., Horvath, J., Zariwala, M.A., Fliegauf, M., Loges, N.T., Wildhaber, J., Noone, P.G., Kennedy, M., Antonarakis, S.E., et al. (2006). *DNAH5* mutations are a common cause of primary ciliary dyskinesia with outer dynein arm defects. Am. J. Respir. Crit. Care Med. *174*, 120–126.
14. Zariwala, M.A., Leigh, M.W., Ceppa, F., Kennedy, M.P., Noone, P.G., Carson, J.L., Hazucha, M.J., Lori, A., Horvath, J., Olbrich, H., et al. (2006). Mutations of *DNAI1* in primary ciliary dyskinesia: evidence of founder effect in a common mutation. Am. J. Respir. Crit. Care Med. *174*, 858–866.
15. Zariwala, M., Noone, P.G., Sannuti, A., Minnix, S., Zhou, Z., Leigh, M.W., Hazucha, M., Carson, J.L., and Knowles, M.R. (2001). Germline mutations in an intermediate chain dynein cause primary ciliary dyskinesia. Am. J. Respir. Cell Mol. Biol. *25*, 577–583.
16. O'Roak, B.J., Deriziotis, P., Lee, C., Vives, L., Schwartz, J.J., Girirajan, S., Karakoc, E., Mackenzie, A.P., Ng, S.B., Baker, C., et al. (2011). Exome sequencing in sporadic autism spectrum disorders identifies severe de novo mutations. Nat. Genet. *43*, 585–589.
17. Day, A., Carlson, M.R., Dong, J., O'Connor, B.D., and Nelson, S.F. (2007). Celsius: a community resource for Affymetrix microarray data. Genome Biol. *8*, R112.
18. Day, A., Dong, J., Funari, V.A., Harry, B., Strom, S.P., Cohn, D.H., and Nelson, S.F. (2009). Disease gene characterization through large-scale co-expression analysis. PLoS ONE *4*, e8491.
19. Takada, S., Wilkerson, C.G., Wakabayashi, K., Kamiya, R., and Witman, G.B. (2002). The outer dynein arm-docking complex: composition and characterization of a subunit (oda1) necessary for outer arm assembly. Mol. Biol. Cell *13*, 1015–1029.
20. Olbrich, H., Häffner, K., Kispert, A., Völkel, A., Volz, A., Sasmaz, G., Reinhardt, R., Hennig, S., Lehrach, H., Konietzko, N., et al. (2002). Mutations in *DNAH5* cause primary ciliary dyskinesia and randomization of left-right asymmetry. Nat. Genet. *30*, 143–144.
21. Gray, T.E., Guzman, K., Davis, C.W., Abdullah, L.H., and Nettesheim, P. (1996). Mucociliary differentiation of serially passaged normal human tracheobronchial epithelial cells. Am. J. Respir. Cell Mol. Biol. *14*, 104–112.
22. Fulcher, M.L., Gabriel, S., Burns, K.A., Yankaskas, J.R., and Randell, S.H. (2005). Well-differentiated human airway epithelial cell cultures. Methods Mol. Med. *107*, 183–206.
23. Ostrowski, L.E., Blackburn, K., Radde, K.M., Moyer, M.B., Schlatzer, D.M., Moseley, A., and Boucher, R.C. (2002). A proteomic analysis of human cilia: identification of novel components. Mol. Cell. Proteomics *1*, 451–465.
24. Ostrowski, L.E., Thompson, K., Blackburn, K., and Goshe, M. (2011). Identification of novel protein that are highly expressed in human cilia by quantitative proteomics. Am. J. Respir. Crit. Care Med. *183* (A1224).
25. Zhou, H., Wang, X., Brighton, L., Hazucha, M., Jaspers, I., and Carson, J.L. (2009). Increased nasal epithelial ciliary beat frequency associated with lifestyle tobacco smoke exposure. Inhal. Toxicol. *21*, 875–881.
26. Becker-Heck, A., Zohn, I.E., Okabe, N., Pollock, A., Lenhart, K.B., Sullivan-Brown, J., McSheene, J., Loges, N.T., Olbrich, H., Haeffner, K., et al. (2011). The coiled-coil domain containing protein CCDC40 is essential for motile cilia function and left-right axis formation. Nat. Genet. *43*, 79–84.
27. Merveille, A.C., Davis, E.E., Becker-Heck, A., Legendre, M., Amirav, I., Bataille, G., Belmont, J., Beydon, N., Billen, F., Clément, A., et al. (2011). CCDC39 is required for assembly of inner dynein arms and the dynein regulatory complex and for normal ciliary motility in humans and dogs. Nat. Genet. *43*, 72–78.
28. Panizzi, J.R., Becker-Heck, A., Castleman, V.H., Al-Mutairi, D.A., Liu, Y., Loges, N.T., Pathak, N., Austin-Tse, C., Sheridan, E., Schmidts, M., et al. (2012). *CCDC103* mutations cause primary ciliary dyskinesia by disrupting assembly of ciliary dynein arms. Nat. Genet. *44*, 714–719.
29. Blanchon, S., Legendre, M., Copin, B., Duquesnoy, P., Montantin, G., Kott, E., Dastot, F., Jeanson, L., Cachanado, M., Rousseau, A., et al. (2012). Delineation of *CCDC39/CCDC40* mutation spectrum and associated phenotypes in primary ciliary dyskinesia. J. Med. Genet. *49*, 410–416.
30. Loges, N.T., Olbrich, H., Fenske, L., Mussaffi, H., Horvath, J., Fliegauf, M., Kuhl, H., Baktai, G., Peterffy, E., Chodhari, R., et al. (2008). *DNAI2* mutations cause primary ciliary dyskinesia with defects in the outer dynein arm. Am. J. Hum. Genet. *83*, 547–558.
31. Schwarz, J.M., Rödelsperger, C., Schuelke, M., and Seelow, D. (2010). MutationTaster evaluates disease-causing potential of sequence alterations. Nat. Methods *7*, 575–576.